Facies analysis of the Middle Cretaceous Mishrif Formation in southern Iraq borehole image logs and core thin-sections as a tool

Maher J. Ismail [a], Frank R. Ettensohn [b], Amna M. Handhal [b,c], Alaa Al-Abadi [b,c,*]

[a] *Basra Oil Company, Basra, Iraq*
[b] *Department of Earth and Environmental Sciences, University of Kentucky, USA*
[c] *Department of Geology, College of Science, University of Basrah, Basrah, Iraq*

ARTICLE INFO

ABSTRACT

The Middle Cretaceous Mishrif Formation is one of the most important oil reservoirs in central and southern Iraq. The major goal of this study is to calibrate the FMI imaging log in front of the depth intervals where core data is available (thin sections), and then utilize the calibrated FMI behavior to predict the types of microfacies in the wells where core data is not available. Hence, this study focuses on distinguishing and correlating carbonate facies in four wells from the Mishrif Formation in the West Qurna and North Rumalia oilfields, southern Iraq, using borehole image logs and thin sections. Thin-section data from the cored wells were used to identify six carbonate environments based on their constituent carbonate microfacies and grain types. A succession of carbonate-environment-facies units was determined in the cores relative to already established members (mB2, mB1, CRII, mA, CRI) and used to discern how the borehole image logs respond to respective carbonate facies. These borehole image responses to changing carbonate-facies units were then used to identify similar behaviors in the wells without core and for correlation across the two oilfields. Thin-section analysis of microfacies and grain types led to the interpretation of six carbonate-environment facies in the Mishrif Formation, including mid-ramp, shoal, back-shoal, lagoonal and intertidal facies; a rudist-bioherm subfacies also occurred locally in shoal, back-shoal, and lagoonal facie units. The organization of the carbonate-environmental-facies units and their correlation across the two oilfields confirms that the Mishrif Formation in southern Iraq comprises two progradational depositional cycles, separated by a major transgressive flooding surface. Clearly, the combined analyses of thin sections from cored wells and borehole image responses from the same wells provide a powerful tool in understanding and correlating facies and sequences across nearby oilfields.

1. Introduction

Borehole imaging is one of the fastest and most reliable techniques for gathering subsurface data (Poppelreiter et al., 2010). Increasingly, borehole imaging has been integrated into reservoir models while drilling, which is an important step toward real-time field optimization (Sparkman, 2003). Types of borehole imaging devices include electrical, acoustic, and video, and these devices are currently available for both wireline and logging-while-drilling environments for use in both open-hole and cased wells (Prensky, 1999). The Fullbore Formation MicroImager (FMI), which was used in this study, is an electrical device that is a powerful and very effective tool in capturing electrical images of the well wall with a strong ability to discriminate and an excellent

degree of coverage. The image's resistivity contrast is expressed by various colors, with dark colors reflecting measurements of low resistivity and bright colors representing measurements of high resistivity (Slim, 2007). The FMI provides a means of understanding geologic environments through borehole images of rock, from carbonate systems with large voids (karstic) to thinly laminated forms. Linear features that intersect the borehole show as sinusoids in the image, which spins from 0° to 360°. The images are frequently orientated to the geographic north so that the sinusoids' peaks and troughs can be connected sequentially to the dip and azimuth of the relevant features. For this reason, the images captured by these logs provide information about the formation encountered that other petrophysical logs cannot provide. Bedding, fractures, faults, stratigraphic features, and a variety of other properties

may all be recognized manually or semi-automatically, and their orientations computed fast. Borehole imaging technologies are frequently employed in conjunction with thorough core analysis for a variety of different purposes, including sequence stratigraphy, facies architecture, and digenetic study (Aghli et al., 2014). Borehole imaging has lately become popular for assessing reservoir characteristics and determining the impact of depositional and diagenetic factors on porosity development and permeability heterogeneity in carbonate systems (Akbar et al., 1995). Image logs have been utilized for different quantitative studies in carbonate reservoir characterization, notably in porosity and permeability assessments of vuggy carbonate reservoirs, in addition to their application in sedimentary interpretation (Chitale et al., 2010). With dual porosity systems in carbonates, Newberry et al. (1996) devised a method for converting electrical pictures into borehole porosity maps, allowing the separation of primary (matrix) and secondary (vuggy) kinds of porosity. (↑Russell et al., 2002) introduced a methodology for characterizing and extrapolating the degree of geological heterogeneity for estimating permeability utilizing electrical, borehole image logs, and conventional log data. Image analysis and enhancement techniques are also available to identify various formation characteristics, including sedimentologic and stratigraphic features, thin-bed description, potential secondary-porosity identification, fracture analysis, and fault mapping (Schlumberger, 2003).

In this study, the sedimentary facies and depositional environments of the Middle Cretaceous Mishrif Formation were studied using borehole image logs acquired from an FMI imaging tool. This research examines the Mishrif carbonate system using a combination of microfacies thin-section analysis and borehole imaging, and gives an explanation for the micro-to meter-scale variations in depositional and diagenetic features that govern reservoir parameters in the considered reservoir unit. The main aim was to calibrate the FMI imaging log in front of the depth intervals in which the core data is available (thin sections) and then use the calibrated FMI behavior to estimate the types of microfacies in the wells that do not contain core data.

2. Geological setting

The West Qurna and North Rumaila oilfields are located in southern Iraq, about 70-km northwest and 50-km west of Basrah city, respectively. The West Qurna Oilfield is located about 14 km from Qurna District, north of Basrah Governorate (Fig. 1). This oilfield is just north of the giant North Rumaila Oilfield in southern Iraq. Structurally, the West Qurna Oilfield is a part of a long-axis anticline. The anticline generally trends N–S, but the trend changes in northern parts of the field to NW-SE. The West Qurna flank dip is slightly asymmetrical with the eastern flank dipping at about 1.6°, whereas the west flank's dip varies from 2° to 3.5°. The West Qurna Oilfield is about 40-km long and 17-km wide. The field occurs on the outer platform of the Arabian Plate in the Mesopotamia foredeep basin (Fouad, 2010). The adjacent North Rumaila Oilfield also reflects a nearly N–S elongated anticlinal trend. The dip on the anticline flanks is around 3°, but the western flank is slightly steeper than the eastern flank, and the anticline is slightly asymmetrical. The entire structure at North Rumaila is approximately 42– km long and 11–km wide, sloping gently southward to form a saddle separating it from the South Rumaila Oilfield (Al-Ansari, 1993).

The Mishrif Formation is widespread throughout the Arabian Peninsula and contains a shallowing-upward succession (Ali et al., 2013; Al-Musawi et al., 2020) of shallow-water, shelf carbonates composed of bioclastic limestones, including in places algal, coral, and rudist bioherms deposited during a 3 my period (Sharland et al., 2004). In the Middle east, mud-dominated Cretaceous platforms developed on the NE margin of Arabian Plate and provided important microporous reservoir (Mehrabi and Rahimpour-Bonab, 2014; Mehrabi et al., 2020; Bagherpour et al., 2021). The Mishrif Formation is regarded as the most important oil reservoir in the Mesopotamian Basin. It is part of the second-order systems tract that ranges from the uppermost Albian to the
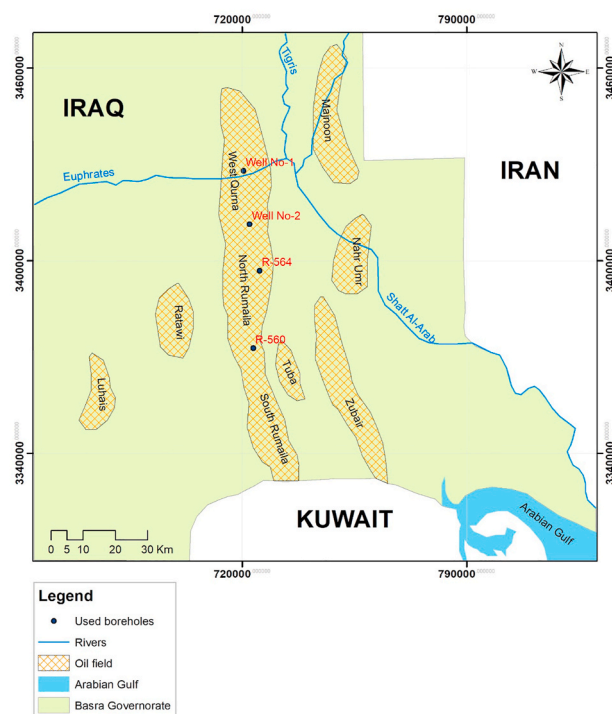

Fig. 1. Location of Oilfields in southern Iraq and the cored holes used in this study.

Turonian and falls within the upper part of the Arabian Plate Mega Sequence 8, AP8, Fig. 2 (Simmons et al., 2007). The underlying Ahmadi and Rumaila formations along with the Mishrif Formation form part of the highstand systems tract for the upper part of the second super sequence IV (Fig. 2). The underlying Rumaila Formation consists mostly of chalky and marly limestones that grade conformably into the Mishrif Formation (Al-Ameri et al., 2009). The Mishrif Formation in southern Iraq represents part of a large carbonate platform system that covered the Arabian Plate from Iraq to Oman. The formation is Late Cretaceous (Cenomanian–Early Turonian) in age, although in local terminology, it is part of an unconformity-bound, uppermost Aptian–lower Turonian sequence that is commonly placed in Middle Cretaceous Series (Fig. 2). Within the Iraqi Mesopotamian Basin, the formation is one of the most productive hydrocarbon reservoirs of many regional oilfields (Al-Musawi et al., 2018; Mahdi and Aqrawi, 2014), including the world-class super-giant hydrocarbon accumulation in the West Qurna Oilfield. The formation comprises thick carbonates of middle Cenomanian – early Turonian age deposited on a basin-wide shallow-water platform, which in the study area experienced uplift on the Amara paleo-high during deposition (Aqrawi et al., 1998). Based on fossils found in a variety of microfacies, depositional environments represented by the Mishrif Formation include sub-basinal, lagoonal, open shelf margin, and shoal (Chafeet et al., 2020). The thickness of the formation is about 200 m, and it is subdivided into several informal members in order top to bottom: CRI, mA, CRII, mB1, and mB2. The most oil prolific reservoir member is the upper mB2 in the West Qurna and North Rumaila oilfields. The CRII non-reservoir zone acts as a laterally continuous flow barrier across the field area and separates mA from mB1.

3. Material and methods

As a major part of this study, 200 thin sections of limestone samples from the Mishrif Formation were examined using a polarizing microscope to determine the texture and microfacies and to classify the components and processes of diagenesis. The allochemical constituents were identified using the skeletal and nonskeletal grain characters of

System/ Series		Group	Formation	Lithology	Discription	Thickness (m)	Mega sequence	Super sequnce
Quaternary	Pleistocene		Q. Deposits		Clay with Gypsum.	180		
Tertiary	Miocene	Kuwait Group	Dibbdiba		Sand / Gravel.	220	Ap11	IV
			Fataha		Marl and/or Limestone.	120		
			Ghar		Sand / Gravel & Sandstone.	90		III
	M-L Eocene	Hasa Group	Dammam		Dolomite.	220	Ap10	I
	Paleocene-E Eocene		Rus		Anhydrite.	60		
			Umm-Radummuah		Dolomite with dolomitic Lst and Anhydrite.	450		
Cretaceous	Upper Cretaceous	Aruma Group	Tayarat		Dolomite interbedded with Anhydrite.	260	AP9	VI
			Shiranish		Limestone intebedded with Marl.	105		
			Hartha		Limestone intrbedded with Dolomite.	190		
			Sadi		Chalky Argillaceous Limestone.	240		V
			Tanuma		Shale.	45		
			Khasib		Argillaceous Chalky Limestone with Shale.	60		
	Middle Cretaceous	Wasia Group	Mishrif		Limestone.	140	AP8	IV
			Rumaila		Argillaceous Chalky Limestone.	90		
			Ahmadi		Shale & Limestone interbeds.	140		
			Mauddud		Limestone.	110		III
			Nahr Umr		Sandstone interbeded with shale.	260		
	Lower Cretaceous	Thammama Group	Shuaiba		Limestone and Dolomite.	80		II
			Zubair		Sandstone & Shale.	425		
			Ratawi		Shale & Limestone interbeds.	260		
			Yammama		Limestone.	280		I
Jurassic	Upper Jurassic		Sulaiy		Limestone with some Shale.	245		

Fig. 2. Stratigraphic column in the south of Iraq (work of authors based on data form the Basrah Oil Company).

Flügel (2012), and samples were classified using the nomenclature of Dunham (1962) and Embry and Klovan (1971). These thin sections were interpreted as to depositional environment using the models of Burchette and Wright (1992), and these environments were related to segments of the core and compared with their respective FMI image analyses in four wells. The four wells include No. 1 and No. 2 from the West Qurna Oilfield and R-564 and R-560 from the adjacent North Rumaila Oilfield (Fig. 1).

The FMI, manufactured by Schlumberger, is a wireline-based micro-resistivity formation imager developed for use with fresh water-based muds. This instrument creates a high-resolution borehole picture (0.2 inches; 0.5 cm) with an 80 percent borehole coverage in 8-inch (20.3 cm) wells using 192 micro-resistivity buttons dispersed along four pads and flaps (Schlumberger, 2002). Borehole images are delivered to various phases of a processing workflow. The speed correction and image orientation, as well as the use of high-resolution accelerometer and magnetometer data, a color mapping scale of resistivity values, and the use of filtering/enhancements to eliminate non-geological artifacts, are the most significant components of the procedure. Artifacts from logging activities, borehole well characteristics (e.g., rugosity, washout, breakouts), processing (e.g., pad mismatching), and the geological formation's composition can all impact image quality. Typically, borehole images are presented in an "uncovered borehole" format with the cylindrical borehole surface log opened to the north azimuth and unrolled to a flat strip, on which straight dipping surfaces are epitomized by sinusoids (Rider, 1986).

Borehole image log interpretation provides structural information and directional sedimentology, which may be used to provide high-resolution data for reservoir interpretation and geomechanical models. The sedimentary interpretation of electrical image logs follows

procedures similar to those used in strictly sedimentological analysis, building up via lithology, texture, and sedimentary structures into facies and then sequences (Rider, 1986). It should, however, be recognized that any information from downhole images reflects the combined electrical response to downhole variations in mineralogy, texture, pore systems, and fluids. In this study, borehole image facies from four wells in the West Qurna and North Rumaila oilfields were analyzed for comparative carbonate facies using thin sections from two of the wells which had cores.

3.1. Imager log response

The electrical image response is the key to interpreting and understanding the behavior of the logging tool relative to the rock and fluid characteristics. The FMI images are mainly focused on sedimentary interpretations at the energy level of the depositional system (Shahinpour, 2013). Color patterns in the FMI images typically reflect the architecture of the rock, and below are listed some common logging image responses:

Resistive: With conventional logging tools, a resistive log response reflects the high resistivity values from materials like hydrocarbons or the low-porosity matrices (non-invaded and resistive materials) like anhydrite. Usually, resistive materials are reflected in light colors, starting with white (Wilson et al., 2013).

Conductive: In conventional logs, low resistivity values are recorded in marls, clays, and shales. In image logs, they are represented by darker colors (often black). However, vugs or high-porosity zones are also reflected as conductive when saturated with drilling fluids.

Mottled: Mottles may reflect as the alternation of resistive and conductive patterns in response to various grain sizes (Wilson et al., 2013). Irregularly shaped mottles indicate a moderate-energy grain

association, whereas coarse mottles are interpreted to reflect grain associations from moderate-to high-energy environments. Mottled-image facies represent a range of microfacies, including bioclastic packstone, coral floatstone, rudstone, and breccias with clasts or bioclasts of variable sizes. The size of the mottles reflects the size of the skeletal bioclasts, with large mottles reflecting large benthic shells as resistive reflections in a high-porosity, conductive background. On the other hand, a conductive background with resistive grains may reflect a high-porosity background with carbonate grains invaded by drilling fluids. Large mottles typically mark large bioclastic skeletal grains in the porous matrix.

Laminated: This image pattern shows thin, rhythmically layered conductive and resistive patterns of relatively uniform thickness. Typically, laminated-image facies are observed in low-energy environments with mudstone and wackestone microfacies predominating. Rare bioclast fragments are observed in the argillaceous limestone deposits from the restricted environments represented by this pattern (Al-Awadi et al., 2017).

Bedded: Intervals of conductive or resistive patterns bounded by horizontal surfaces. The thickness of the bedded patterns ranges from many centimeters to several meters. This FMI bedded facies images consist of medium-to thick-bedded, resistive limestone beds with fine interbedded conductive materials (Amer et al., 2011). In the bedded limestone, FMI image facies correspond to planktic foraminiferal packstones interbedded with bioclastic packstones, containing fragmented shallow-water bioclasts.

4. Results

4.1. Microfacies type from the cross-sections

Examine the available thin-sections have been showed that the Mishrif Formation comprises the following main microfacies (Fig. 3):

- *Mudstones* – the grains are floating in the matrix. The rocks comprise 10% of grains with the size of 0.3–2.0 mm. Mudstones indicate low-

to very low-energy environments. Sedimentation of such rocks occurred in the places protected from the sea currents. The mudstone microfacies had been seen in supratidal environment with rare bioclasts fragments. Also, the mid-ramp environment has the mudstone microfacies with planktonic foraminifera.

- *Wackestones* –the grains have the size of 0.3–2.0 mm, and are 'floating' in the matrix. Their percent content in the rocks amounts to 10% and more. Wackestone represent mainly low-energy depositional settings with limited grain-producing organisms. A wackestone had identify in verity environments as the mid ramp environment which contained the barrows shells, coral fragments, echinoderms fragments, and rudist fragments. The back-shoal and lagoon environments have also the wackestone microfacies that contained the benthic foraminifera, coral, echinoderms, rudist, algal fragments.

- *Packstone* – the texture is supported by the grains with the size of 0.3–2.0 mm, which contact each other and form the rigid frame. The intergranular space is filled with the fine-grained matrix. Packstone were deposited next to shoals and the areas of the active hydrodynamics. The packstone microfacies identify in mid-ramp environment that contained Mollusca, brachiopods, pelecypods shells with allochem fragments like echinoderms, rudist fragments. This microfacies showed in shoal and rudist bioherm environments beside the grainstone and rudstone microfacies. Benthic foraminifera packstone is common microfacies in lagoon and back-shoal environments.

- *Grainstone* – consist of grains with the size of 0.3–2.0 mm. Grainstone include the rocks, in which the fine-grained carbonate material (matrix) is absent, and the grains compose the rigid frame resting on each other. The inner-granular space is free and made of cement. Grainstone were formed in a very active hydrodynamic environment. They are typical for the wave area of extremely shallow water, associated with the extreme shallow areas of reef systems. The grainstone microfacies usually characterized the shoal and rudist bioherm environments which have high energy level and large bioclast fragments size.
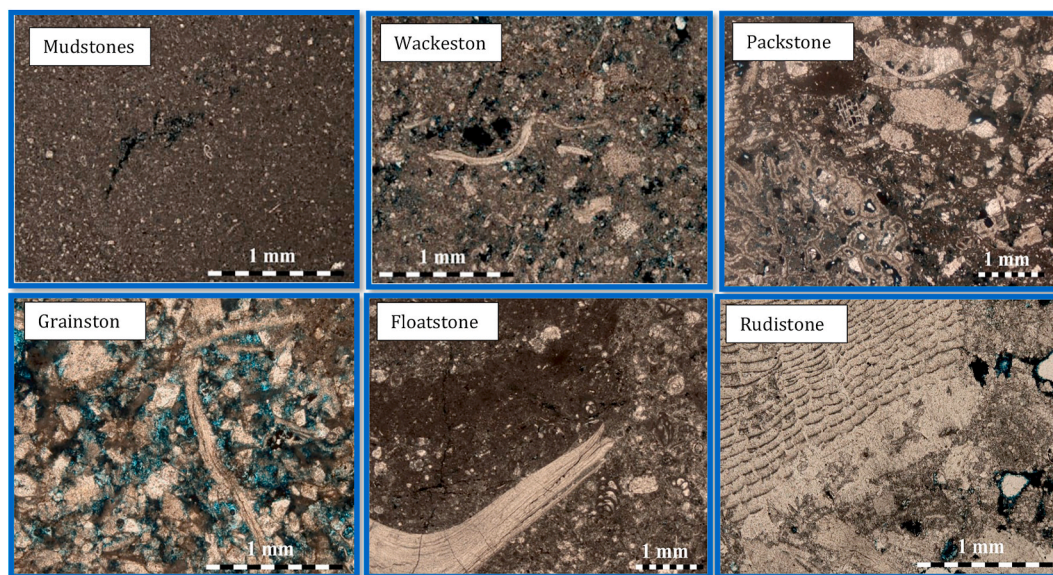

Fig. 3. Type of microfacies in the study area at well No.1; depth: 2569 = mudstone, depth: 2463 = wackestone, depth: 2423 = packstone, depth: 2437 = grainstone, depth: 2467 = Floatstones, depth: 2420 = rudistone.

- *Floatstones* **–** the rocks contain above 10% of grains with the size of 2 mm and more. The grains are 'floating' in the fine-grained matrix. Floatstones were deposited in the calm environment on the slopes controlling the high areas of terrain and reef systems.
- *Rudistone* – large size fragments rocks, where the grains with the size of > 2 mm contact each other, making the rigid frame. The inner-granular space is either free or covered with cement or rarely with the fine-grained matrix. Rudistone, as well as packstone, control the terrain, but mainly its shallower parts (outside slopes and top surfaces of reef systems). Such rocks are typical for the areas with the active hydrodynamic mode.

4.2. Lithofacies associations

The combined study of thin sections and corresponding image-log analysis from the Mishrif Formation in the study area revealed six facies (Fig. 4):

1) **Mid-ramp and open-marine environment:** Wackestones to wack-epackstones that are matrix-rich and often fine-grained. Locally common argillaceous seams have been compacted and/or bioturbated. Bivalve and echinoderm debris with benthic foraminifera and locally common planktonic foraminifera make up the fauna.

   Interpretation: Low-energy open marine-influenced context with
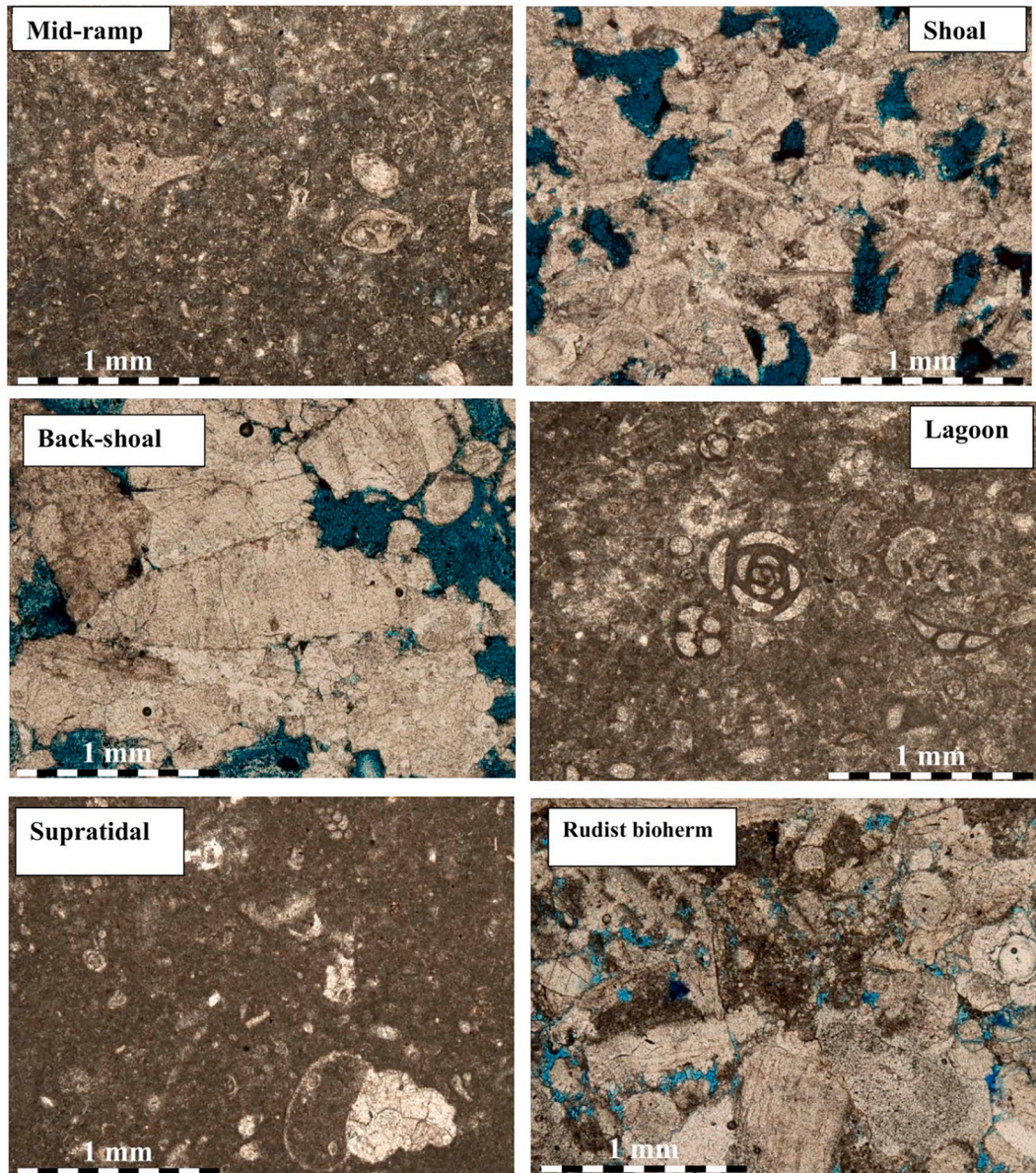

Fig. 4. Thin sections showing lithofacies characteristics of depositional environments within the Mishrif Formation from the West Qurna Oilfield, southern Iraq. The blue areas in the thin-section photographs reflect porosity. (For interpretation of the references to color in this figure legend, the reader is referred to the Web version of this article.)

intermittent shoal and lagoon debris reworking during uncommon storms.

2) **Rudist bioherm**: Rudist-rich rudstones and floatstones that have been poorly sorted. Rudists are present, probably in situ and reworked locally. Rarely developed, it can be found in enormous beds with little bioturbation.

Interpretation: Rudist, with a moderate to high level of energy. Reservoir quality has the potential to be good.

3) **Shoal**: Packstones to grainstones with erosive surfaces, graded bedding, and low-angle lamination. Sorted echinoderm fragments, peloids, coated grains, benthic foraminifera, algal debris, and

intraclasts dominated the grains. Bioturbation and argillaceous seams are uncommon.

Interpretation: Moderate to high-energy sediment transport within movable shoals dominated by currents. Some of the best reservoir quality can be found here.

4) **Back-shoal**: Wackestones that are primarily grain-rich, with minor floatstones, have a variable connection with packstones. Coated grains, peloids, intraclasts, and skeletal detritus of echinoderms, rudists and other bivalves, green algae, and benthic forams make up the diverse grain assemblage. Variable vertical organization with argillaceous intervals, ranging from upward-cleaning to upward-dirtying.
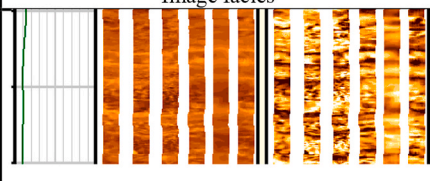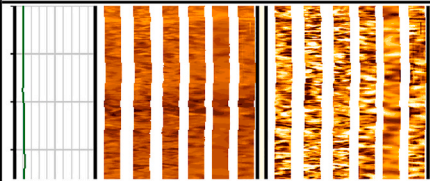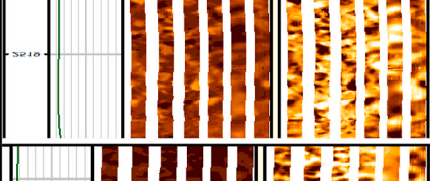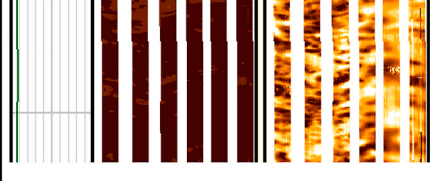
Environment	Image facies	Log response	Interpretation
Intertidal		**Conductive, laminated**	Small-scale, conductive lamination due to low energy level and rare bioclast content, conductive dark laminated electrical reflections with resistive thin beds alternating on a centimeter scale.
Lagoon		**Small-scale conductive, mottled**	Conductive background with small-scale mottles due to low energy, with small skeletal bioclasts of benthic foraminifera and bivalve fragments.
Back-shoal		**Mottled**	Conductive background with mottled shapes due to cemented carbonate with clay content; larger resistive mottles reflect in diagenetically cemented carbonate grains.
Shoal		**Conductive, mottled**	Mottled conductive and resistive alternation refers to rich content of skeletal bioclasts of fragmented echinoderms, rudist clams and bivalve fragments; high-energy levels and absence of laminae
Rudist bioherm		**Large-size mottles**	Conductive background with resistive grains due to highly porous nature and invasion by drilling fluid inside the formation; the large size of resistive mottles reflects the size of bioclast fragments.
Mid-ramp		**Resistive, bedded**	Light conductive background with resistive small-scale mottles due to low energy levels Bioclast fragments less than shoal, planktonic foraminifera.
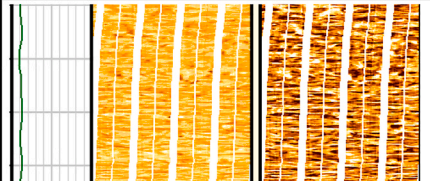
Fig. 5. FMI Image facies summary diagram with environmental interpretations.
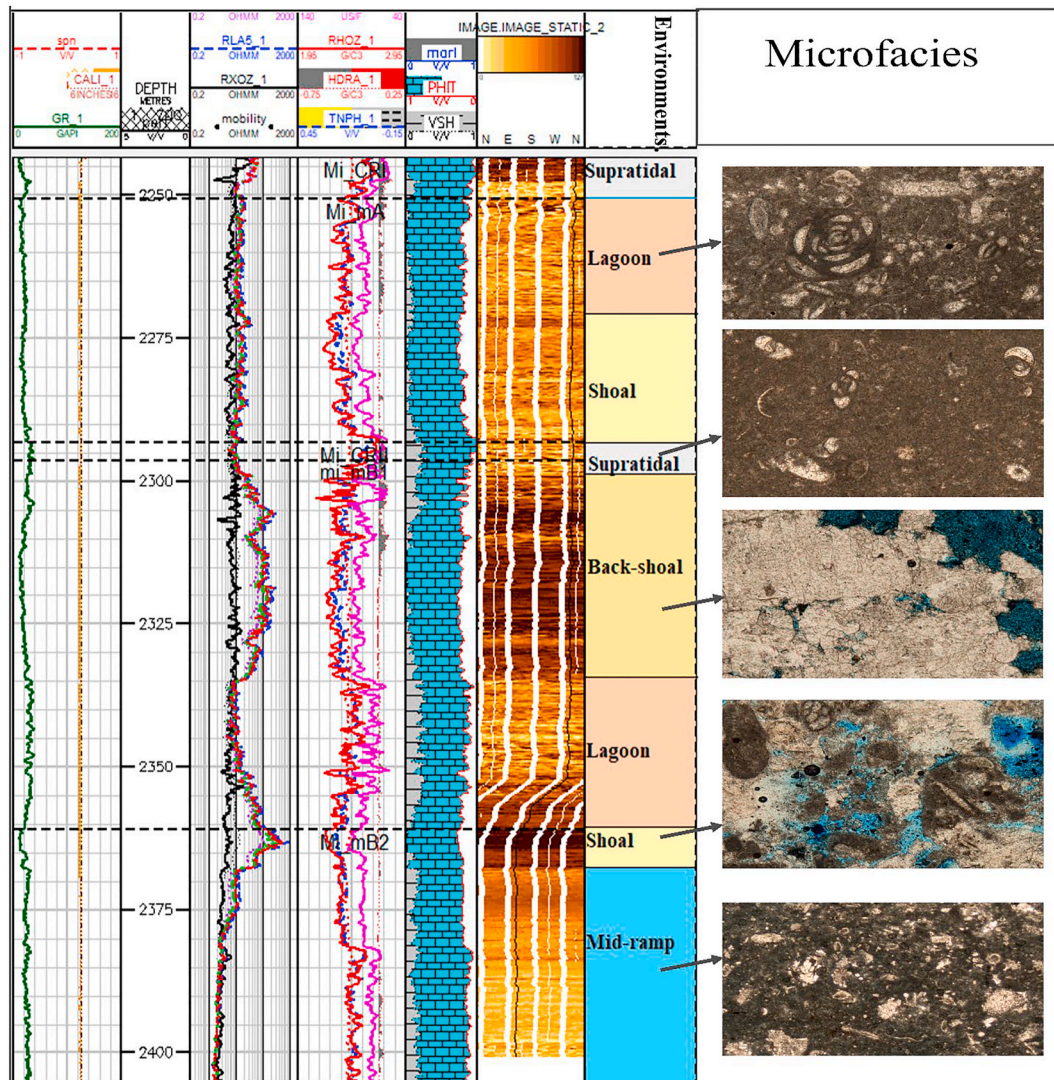
Fig. 6. Relationship between logging responses, FMI Image facies variation, and thin-section samples (microfacies) from different environments represented in well R-564 from the North Rumaila Oilfield. Blue coloration in thin sections reflects porosity. (For interpretation of the references to color in this figure legend, the reader is referred to the Web version of this article.)

Interpretation: Storm reworking in back shaol settings to less energetic lagoon floor deposits is characterized by shallow water, low to moderate energy. Reworking is seen in the variety of fanua and texture. Sedimentation rates range from low to moderate, with high concentrations in some areas.

5) **Lagoon:** Rare floatstones in bioturbated wackestone to packstone. Benthic foraminifera and thin-shelled bivalves have a limited fauna. Upward cleaning units are formed.

Interpretation: low-energy scenario in a lagoonal environment with limited resources.

6) **Intertidal**: Wackestones to wackepackstones with minimal packstone and microbiological boundstone textures are dominant.

Miliolid forams and thin-shelled bivalves with reworked skeletal debris, intraclasts, and blackened grains are common in this area. Cleaning and dirtying ascending cycles are organized vertically into m to sub-m scales.

Interpretation: a low-energy depositional environment with a high salt level (restriction). High-energy events occurred on a frequent basis, transporting reworked lagoon material into the setting. Due to shallow water depths and susceptibility to relative sea level change, the environment was prone to periodic sedimentation breaks.

Fig. 7 summarizes and interprets the image responses of the FMI for the six Mishrif environments in the study area, whereas Table 1 shows the relationship of facies type with the environment by the response of the image log.
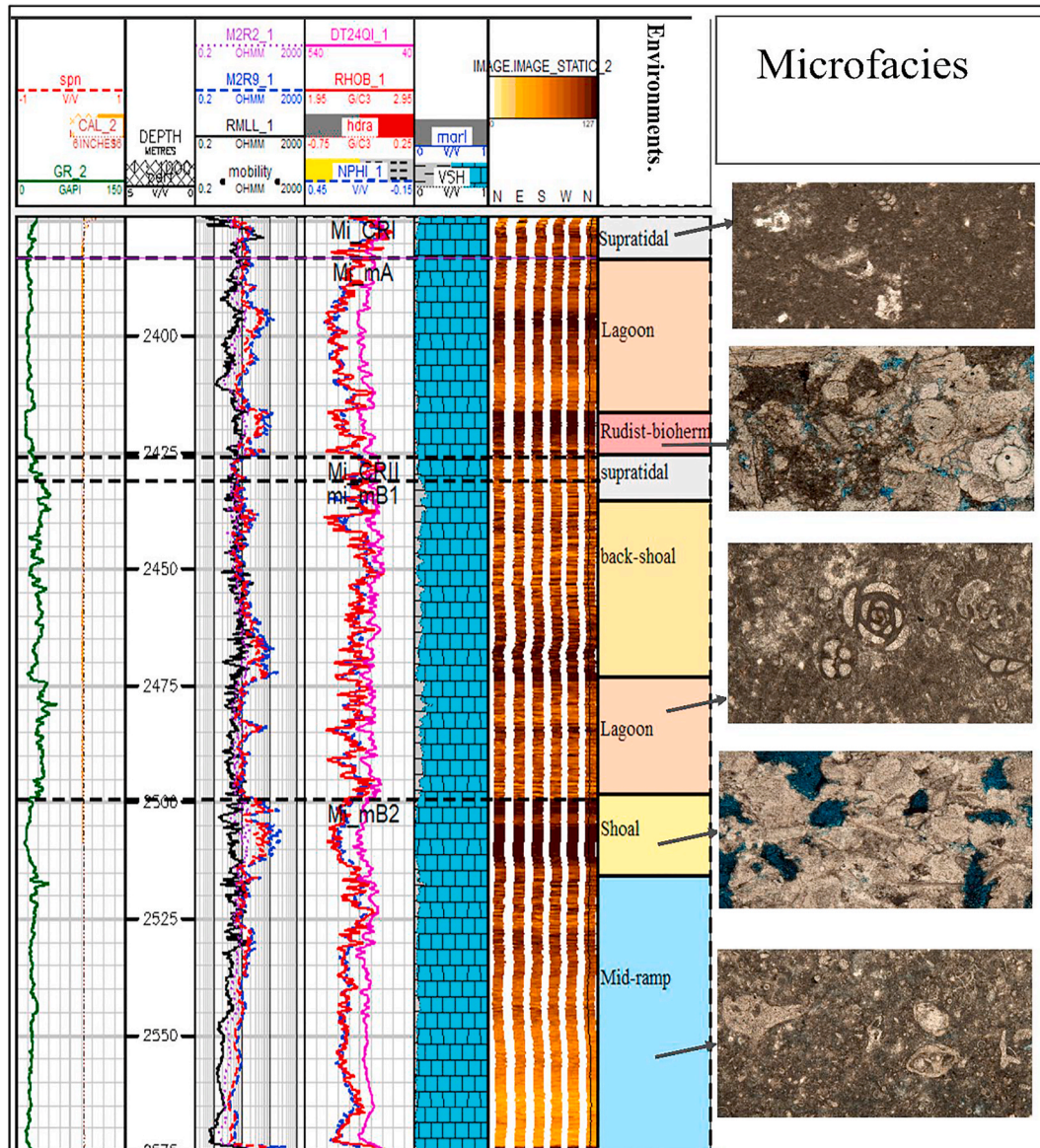
Fig. 7. Relationship between logging responses, FMI Image facies variations, and thin-section samples (microfacies) of different environments from well No.1 of the West Qurna Oilfield, southern Iraq.
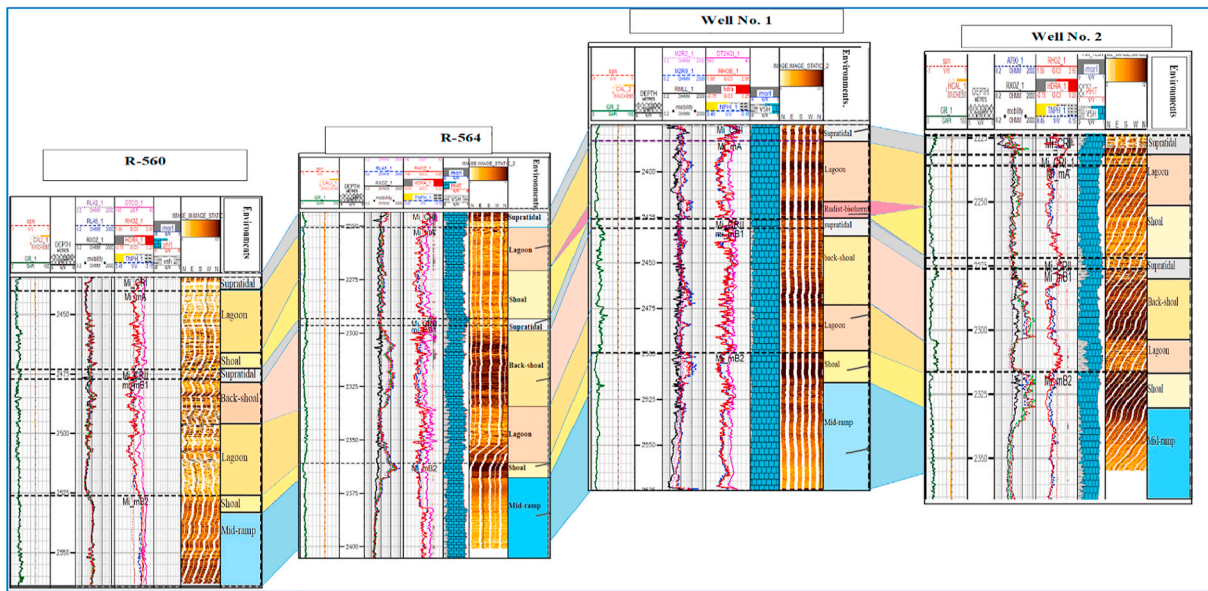
Fig. 8. Correlation between the four wells from the West Qurna and North Rumaila oilfields in the southern Iraq study area.
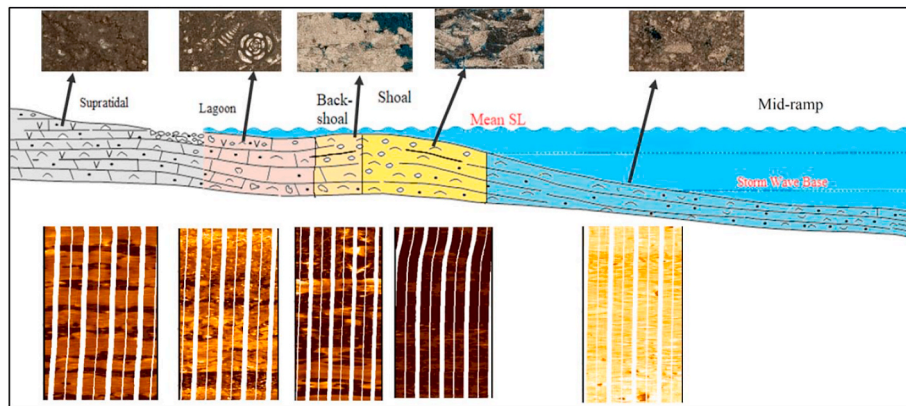

Fig. 9. Depositional model, showing standard carbonate facies belts with the related FMI Image facies responses below, for the Mishrif Formation in the study area.

Table 1
The relationship of facies type with the environment by the response of the image log.

Microfacies	Description	Environments	Image log response
Mudstone + wackestone	Intertidal facies are dominated by bioturbated skeletal wackestone and rare mudstone facies. intertidal facies interbedded skeletal packstone with wackestone and argillaceous prone mudstone and wackestone.	Intertidal	Small scale conductive laminated due to low energy level and rare bioclast contents, conductive black laminated electrical reflection with resistive thin beds alteration with cm scale.
Wackestone + packstone	skeletal peloids wackestone, wacke-packstone, and packstone fabric. Low assemblages of fauna contained benthic foraminifera including Miliolids	Lagoon	Conductive background with small scale mottled due to low energy, with small skeletal bioclast benthic foraminifera and bivalves' fragments.
Wackestone + packstone	skeletal peloids packstone, wackestone, and floatstone with few grainstone. Echinoderms, bivalves, benthic foraminifera, green algal, and rudist are the common bioclast skeletal	Back-shoal	Conductive background with mottled shapes due to cemented carbonate with clay content, resistive mottled reflected the cemented carbonate grains fragments.
Packstone + grainstone	Peloidal skeletal packstone to grainstone rudists attitudes, the bioclasts of shoal environments are bivalves, intraclasts, coral, green algal, echinoderms, and rudists shells.	Shoal	Mottled conductive and resistive alternation refers to rich contents of bioclast skeletal echinoderms, rudist and bivalves' fragments, high energy level not laminated beds.
Grainstone + rudstone	Peloidal skeletal rudstone and grainstone rudists attitudes, the bioclasts of bioherm environments are bivalves, intraclasts, coral, green algal, echinoderms, and rudists shells.	Rudist bioherm	Conductive background with resistive grains due to high porous, high invaded drilling fluid inside the formation. the resistive large size mottled reflected the size of bioclast fragments.
Wackestone + packstone	bioclasts fragments, peloids, wackestone, wacke-packstone with very minor floatstone, grainstone. The bioclast fragments are always debris of pelecypods, brachiopods, gastropods, green algal, rudist, echinoderms	Mid-ramp	Light conductive background with resistive small scale mottled due to energy level decreased than shoal. Bioclast fragments less than shoal, planktonic foraminifera.

5. Discussion

1. **Mid-ramp and open-marine environmental facies** (Figs. 4 and 6): This facies represents the lower part of Mishrif Formation (Fig. 6). Mid-ramp deposits contain skeletal debris and peloids in wackestone and wackestone-packstone with very minor amounts of floatstone, grainstone, and boundstone. The skeletal components are more common in proximal parts of the mid-ramp, but not abundant. However, skeletal fragments become less abundant in the distal mid-ramp setting and largely comprise bioclasts of green algae, rudist clams, echinoderms, and benthic foraminifera. On the other hand, the distal part of the mid-ramp and adjacent open-marine environments have a greater abundance of planktic foraminifera. In terms of image analysis, the image facies are resistive to small mottles between the intervals (2517–2574 m) in well No. 1 and (2330–2355 m) in well No. 2. In West Qurna, this facies appears in the interval (2533–3575 m) in well R-560 and in the interval (2367–2400 m) in well R-564 from the North Rumaila Oilfield. In all these intervals, the mid-ramp environment predominated, and the microfacies are wackestone and packstone. The included bioclasts are whole to fragmented rudist shells, irregularly oval peloids, echinoderm fragments, scattered ostracod valves, small foraminiferal tests, and rare small shells of gastropods and brachiopods. Locally, red algae and coralbioclasts predominate in the mid-ramp facies. A ten-centimeter to meter bedded image response is shown and correlated with core data (Fig. 6).

2. **Rudist bioherm** (Fig. 7): This facies represents high-energy levels and contains large skeletal fragments of rudist clams with a rich-grain texture. The rudist facies exhibits poorly sorted coarse grains of rudist clams in skeletal floatstones and rudstones with less rudist-rich packstones. This facies represents inner-ramp deposits adjacent to the mid-ramp within rudist bioherms and/or patch reefs. The abundance of bioherms is usually associated with low accommodation space (Carlucci and Westrop, 2012). A conductive background with large mottles is characteristic of the rudist-bioherm environment due to highly porous limestones and high fluid invasion. This facies association consists of rudist and echinoderm bioclasts in microfacies of grainstone, rudstone, and packstone. This image facies is located in the interval (2416–2425 m) from well No. 1 in the West Qurna Oilfield (Fig. 7).

3. **Shoal facies** (Figs. 4–7): The upper part of the mB2 reservoir unit and the lower part of mA unit of the Mishrif Formation (Fig. 6) represent a shoal environment. Peloidal-skeletal packstones to rudist grainstones, floatstones, and rudstones characterize the shoal facies. The grains are well to moderately sorted, and bioclast grains forming the shoals are largely composed of bivalve debris, echinoderm ossicles, peloids, intraclasts, and benthic foraminifera. These shoals were characterized by moderate to high-energy conditions, and echinoderm grains become more abundant in the higher-energy, well-sorted, up-section intervals with little argillaceous material. Bioturbated fabrics also occur in the shoal facies but are more typical of inner-shoal settings, where the sediment surface is more stable, and the depositional rate is low. Although the shoal association is epitomized by the high-energy reworking of rudist fragments in shallow sandbelt environments, upper parts of the facies become muddier and more argillaceous as the shoal graded shoreward into deeper-water, back-shoal and lagoonal environments. Image logs for shoal environments typically resistive mottles against a conductive background due to an increase larger grains, which generate the mottles. This image facies is located at the interval (2500–2517) in well No. 1, at the intervals (2316–2330) and (2252–2272) in well No. 2 from the West Qurna Oilfield, and in intervals (2526–2533) and (2466–2474) in well R-560 and at the intervals (2360–2367) and (2272–2292) in well R-564 from the North Rumaila Oilfield. The bioclasts in this facies are typically bivalve, echinoderm, and rudist fragments, which occur as parts of peloidal skeletal packstones to grainstones, and rudstones.

Despite the high-energy nature of the shoal environment, the conductive background reflects high fluid invasion of the high-porosity shoal sediments.

4. **Back-shoal facies** (Figs. 4–7): The upper part of informal member mB1 is characterized as a back-shoal environment (Figs. 4 and 6). The back-shoal facies is characterized by skeletal-peloidal packstone, wackestone, and floatstone with a few grainstones. Fragmental echinoderms, bivalves, benthic foraminifera, green algae, and rudist clams are the common skeletal bioclasts in the back-shoal environment (Schlager, 2005). Typically, a back-shoal association is very heterogeneous in fauna and grain size because energy levels vary from low to moderate, being lower than the adjacent shoal but higher than the shoreward lagoon. The overall upward trend is for the facies to become muddier and more argillaceous upward as the facies grades into deeper lagoonal environments. Thinner, argillaceous beds are typically deposited in lower-energy regimes, whereas thicker beds of clean, well-washed sands reflect higher-energy episodes of deposition. Overall, deposition here is sporadic generating periods of sediment starvation where diagenesis may prevail. The back-shoal image facies commonly appear as cemented resistive grains in a conductive background. Diagenetic processes such as solution, in situ bioclast alteration, and cementation result in the largely mottled facies image. These facies are located in intervals 2435–2475 m in well No. 1, (2280–2305 m) in well No. 2, from the ″West Qurna Oilfield and (2478–2497) in well R-560 and (2998–2335) in well R-564 from the North Rumaila Oilfield. Diagenetically cemented packstones and wackestones predominate in the back-shoal environment.

5. **Lagoon facies** (Figs. 4–7): The lower part of informal member mB1 and the upper part of informal member mA are interpreted to represent a lagoon environment (Fig. 6). Skeletal-peloidal wackestone, wacke-packstone, and packstone facies characterize this environment succession. A low-diversity fauna of benthic foraminifera, including miliolids, thin-shelled bivalves, and rare fragmental rudists and green algae characterize the lagoonal environment (Schlager, 2005) with a low-to-moderate energy regime. The lagoonal environment shared some similarities with adjacent environments, but with areas of higher-energy, cleaner sediments where compared with supratidal facies, and with areas of lower-energy, muddier sediments where compared with back-shoal facies. The lagoon environment image facies generally consist of a more conductive background due to an increased clay content with fragmented shells and benthic foraminifera. This facies appears at intervals (2475–2500 m) and (2383–2416 m) in well No. 1, at intervals (2305–2316 m) and (2232–2252 m) in well No. 2, from the West Qurna Oilfield and at intervals (2497–2526 m) and (2440–2466 m) in well R-560, as well as from intervals (2335–2360 m) and (2251–2272 m) in well R-564 from the North Rumaila Oilfield. The image mottles are of small size because of the smaller size of bioclasts in the lagoonal facies compared with the larger grain sizes in the shoal and back-shoal environments.

6. **Intertidal facies** (Figs. 4–7): The term "intertidal" is used here as a generalized term for both intertidal and supratidal facies, which represent the shallowest depositional environments in the Mishrif Formation (Fig. 6). In the supratidal facies, bioturbated, argillaceous, skeletal wackestone and mudstone, which are commonly laminated, predominate and are characterized by a low-abundance and low-diversity fauna of benthic foraminifera, thinly shelled bivalves, and reworked skeletal debris. These facies are consistent with very low-energy settings, but the presence of abundant bioturbation suggests a lack of restriction with marine waters that were still well-oxygenated. Tides, sporadic storms, and marine flooding events provided sporadic periods of high-energy sediment reworking, often followed by periods of low sedimentation. A laminated image facies with rare bioclast content is typical of the intertidal environments. Image patterns reflecting low energy and high clay content appear in

intervals (2375–2383 m) and (2425–2435 m) in well No. 1, in intervals (2272–2280 m) and (2224–2232 m) in well No. 2, in the west Qurna oilfield, and in intervals (2434.5–2440 m), and (2474–2478 m) from well R-560, as well as in intervals (2392–2398 m) and 2245–2251 m) from well R-564 in the North Rumaila Oilfield. Fig. 8 shows how the image responses can be used for correlation between wells in West Qurna and North Rumaila oilfields. Fig. 9 shows the proposed depositional model for the Middle Cretaceous Mishrif Formation in study area, which is very similar to the idealized sequence of standardized carbonate facies belts that commonly develop across a gently sloping shelf atop a platform (e.g., Wilson, 1975).

6. Conclusions

Imaging tools provide excellent means for understanding ancient carbonate depositional environments while providing borehole images of the penetrated rocks. For example, in the Middle Cretaceous Mishrif Formation from the West Qurna and North Rumaila oilfields in southern Iraq, the use of high-resolution borehole images in combination with thin sections from the same penetrated units has enabled the interpretation of carbonate depositional environments and an understanding of image responses. In particular, the thin sections enable the interpretation of borehole image responses, which are reflected in resistive and conductive colors as mottles, laminae, and beds, in terms of the carbonate microfacies and grains that compose them. Inasmuch as the microfacies and included grains reflect distinct carbonate depositional environments that followed each other during progradation and transgression, their borehole image responses also followed each other stratigraphically and can be used for correlation in cross sections.

Using the combination of four borehole image logs and thin sections, along with the standard carbonate-facies-belt model of Wilson (1975), the following interpretations of the subsurface Mishrif Formation in southern Iraq are suggested:

(1) The Mishrif Formation in the studied oil fields represents a carbonate facies belt of mid-ramp to intertidal facies that experienced two progradational depositional cycles separated by a period of rapid transgression, which can be correlated using borehole image logs; the lower depositional cycle, represented by members, mB2 and mB1, is separated from the upper depositional cycle, represented by informal members, mA and CRI, by a major transgressive flooding surface at informal member CRII.

(2) Across the gently dipping Mishrif shelf, mid-ramp environments, represented by burrowed wackestones and packstones with peloids and fragmented bivalve and echinoderm grains, predominate; this environment is represented by bedded, resistive image facies with small mottles reflecting bioturbation and scattered allochemical grains.

(3) The mid-ramp environment is typically followed by a shoal environment, represented by peloidal-skeletal packstone to grainstone and occasional rudstone, containing larger bioclasts of bivalves, echinoderms and rudist clams; this environment is represented by large resistive mottles, reflecting large bioclasts, against a conductive image-facies background indicating fluid invasion of the typically high porosity.

(4) The back-shoal environment, where present, is characterized by varying energy levels, faunas, and grain sizes; packstone and wackestone generally predominate, but the sporadic nature of sedimentation here generates periods of sediment starvation during which diagenesis prevails, leading to scattered intervals of intense cementation and grain alteration; in image facies, the diagenetic cementation generates large, irregular mottles against a generally conductive background, indicating fluid invasion of local porosity.

(5) The lagoonal environment is characterized by argillaceous, skeletal-peloidal wackestone, wacke-packstone, and packstone with a small, low-diversity fauna of benthic foraminifera and thin-shelled bivalves; the image facies consist of a conductive background due to increased clay content with a few small mottles, reflecting decreased bioclast content and the small size of bioclasts.

(6) The various, shoreward, intertidal environments are characterized by laminated, argillaceous, skeletal wackestone and mudstone with a low-abundance, low-diversity fauna of benthic foraminifera and thin-shelled bivalves; the image facies consists of conductive laminae with small, rare mottles, reflecting a small, sparse fauna.

(7) Although not a large-scale environment like those above, rudist bioherms may occur locally in shoal, back-shoal or lagoonal environments; they occur as accumulations of grainstone, rudstone, and packstone in and around colonies of rudist clams and associated echinoderms; the image facies is represented by large resistive mottles, reflecting large rudist fragments, across a conductive background, indicating fluid invasion into the very prous bioherm.

Declaration of competing interest

The authors declare that they have no known competing financial interests or personal relationships that could have appeared to influence the work reported in this paper.

References

Aghli, G., Fardin, H., Mohamadian, R., Saedi, G., 2014. Structural and fracture analysis using EMI and FMI image Log in the carbonate Asmari reservoir (Oligo-Miocene), SW Iran. Geopersia 4 (2). https://doi.org/10.22059/JGEOPE.2014.52717, 169-084.

Akbar, M., Petricola, M., Watfa, M., Badri, M., Charara, M., Boyd, A., Cassell, B., Nurmi, R., Delhomme, J.-P., Grace, M., 1995. Classic interpretation problems: evaluating carbonates. Oilfield Rev. 7.

Al-Ameri, T.K., Al-Khafaji, A.J., Zumberge, J., 2009. Petroleum system analysis of the Mishrif reservoir in the ratawi, Zubair, north and South Rumaila oil fields, southern Iraq. GeoArabia 14, 91–108.

Al-Ansari, R., 1993. The Petroleum Geology of the Upper Sandstone Member of the Zubair Formation in the Rumaila South. Geol. Study. Minist. Oil, Baghdad, Iraq.

Al-Awadi, A.M., Haines, T., Bertouche, M., Bonin, A., Fuchs, M., Deville De Periere, M., Challa, P., Zaidi, S., 2017. Predictability of the sedimentological make-up and reservoir quality in the mauddud formation using FMI logs-A case study from a north Kuwait field. In: SPE Kuwait Oil & Gas Show and Conference. OnePetro.

Al-Musawi, F.A., Idan, R.M., Salih, A.L.M., 2020. Reservoir characterization, Facies distribution, and sequence stratigraphy of Mishrif Formation in a selected oilfield, South of Iraq. In: Journal of Physics: Conference Series. IOP Publishing, p. 12073.

Al-Musawi, F.A., Idan, R.M., Salih, A.L.M., 2018. Reservoir properties and facies distribution of Mishrif formation in Ratawi oilfield, Southern Iraq. In: Conference of the Arabian Journal of Geosciences. Springer, pp. 121–126.

Ali, F.H.M., Ali, Z., Embong, M.K., Azmi, A.A., 2013. Microfacies analysis and reservoir characterisation of late cenomanian to early turonian Mishrif reservoirs, garraf field, Iraq. In: IPTC 2013: International Petroleum Technology Conference. European Association of Geoscientists & Engineers, p. 350.

Amer, A., Glascock, M., Schwalbach, J., Khan, M., 2011. Applied borehole image analysis in complex sedimentological and structural settings: a single well case study. In: SPE Annual Technical Conference and Exhibition. OnePetro, California, USA.

Aqrawi, A.A.M., Thehni, G.A., Sherwani, G.H., Kareem, B.M.A., 1998. Mid-Cretaceous rudist-bearing carbonates of the Mishrif Formation: An important reservoir sequence in the Mesopotamian Basin. Iraq. J. Pet. Geol. 21, 57–82.

Bagherpour, B., Mehrabi, H., Faghih, A., Vaziri-Moghaddam, H., Omidvar, M., 2021. Tectono-eustatic controls on depositional setting and spatial facies distribution of Coniacian–Santonian sequences of the Zagros Basin in Fars area, S. Iran. Mar. Petrol. Geol. 129, 105072.

Burchette, T.P., Wright, V.P., 1992. Carbonate ramp depositional systems. Sediment. Geol. 79, 3–57.

Carlucci, J.R., Westrop, S.R., 2012. Trilobite biofacies along an Ordovician (Sandbian) carbonate buildup to basin gradient, southwestern Virginia. Palaios 27, 19–34.

Chafeet, H.A., Handhal, A.M., Raheem, M.K.H., 2020. MIcrofacies and depositional analysis of the Mishrif Formation in selected wells of Ratawi oilfield, southren Iraq. Iraqi Geol. J. 127–153.

Chitale, V.D., Johnson, C., Entzminger, D., Canter, L., 2010. Application of a modern electrical borehole imager and a new image interpretation technique to evaluate the porosity and permeability in carbonate reservoirs: a case history from the Permian Basin, United States. AAPG special issue. https://doi.org/10.1306/13181289M923410.

Dunham, R.J., 1962. Classification of carbonate rocks according to depositional textures.

Embry, A.F., Klovan, J.E., 1971. A late Devonian reef tract on northeastern Banks Island. NWT. Bull. Can. Pet. Geol. 19, 730–781.

Flügel, E., 2012. Microfacies Analysis of Limestones. Springer Science & Business Media.

Fouad, S.F.A., 2010. Tectonic and structural evolution of the Mesopotamia foredeep, Iraq. Iraqi Bull. Geol. Min. 6, 41–53.

Mahdi, T.A., Aqrawi, A.A.M., 2014. Sequence stratigraphic analysis of the mid-cretaceous Mishrif Formation, southern Mesopotamian Basin, Iraq. J. Petrol. Geol. 37, 287–312.

Mehrabi, H., Bagherpour, B., Honarmand, J., 2020. Reservoir quality and micrite textures of microporous intervals in the Upper Cretaceous successions in the Zagros area, SW Iran. J. Petrol. Sci. Eng. 192, 107292.

Mehrabi, H., Rahimpour-Bonab, H., 2014. Paleoclimate and tectonic controls on the depositional and diagenetic history of the Cenomanian–early Turonian carbonate reservoirs, Dezful Embayment, SW Iran. Facies 60, 147–167.

Newberry, B.M., Grace, L.M., Stief, D.O., 1996. Analysis of carbonate dual porosity systems from borehole electrical images. In: Permian Basin Oil and Gas Recovery Conference. Society of Petroleum Engineers.

Poppelreiter, M., Garcia-Carballido, C., Kraaijveld, M., 2010. Dipmeter and Borehole Image Log Technology: AAPG Memoir 92. AAPG.

Prensky, S.E., 1999. Advances in borehole imaging technology and applications. Geol. Soc. London, Spec. Publ. 159, 1–43.

Rider, M.H., 1986. The Geological Interpretation of Well Logs. Gulf Pub Col, p. 280.

Russell, S.D., Akbar, M., Vissapragada, B., Walkden, G.M., 2002. Rock types and permeability prediction from dipmeter and image logs: Shuaiba reservoir (Aptian). Abu Dhabi. Am. Assoc. Pet. Geol. Bull. 86, 1709–1732.

Schlumberger, 2002. Borehole geology, geomechanics and 3D reservoir modeling. FMI. SMP-5822.

Schlager, W., 2005. Carbonate sedimentology and sequence stratigraphy. SEPM Soc for Sed Geology.

Schlumberger, 2003. Using borehole imagery to reveal key reservoir features. In: Reservoir Optimization Conference, Tehran, Iran.

Shahinpour, A., 2013. Borehole image log analysis for sedimentary environment and clay volume interpretation. Master thesis. Institutt for petroleumsteknologi og anvendt geofysikk. http://hdl.handle.net/11250/240255.

Sharland, P.R., Casey, D.M., Davies, R.B., Simmons, M.D., Sutcliffe, O.E., 2004. Arabian plate sequence stratigraphy–revisions to SP2. GeoArabia 9, 199–214.

Simmons, M.D., Sharland, P.R., Casey, D.M., Davies, R.B., Sutcliffe, O.E., 2007. Arabian Plate sequence stratigraphy: potential implications for global chronostratigraphy. GeoArabia 12, 101–130.

Slim, M.I., 2007. Borehole-image Log Interpretation and 3D Facies Modeling in the Mesaverde Group, Greater Natural Buttes Field. Master thesis. Unpublished, Uinta basin, Utah.

Sparkman, G.W., 2003. Maximizing Value through Real-Time Data Optimization—The '"E-field"'(abs.): AAPG International Conference, Barcelona, Abstract Volume, Spain, September 21-24, 2003.

Wilson, J.L., 1975. Carbonate Facies in Geologic History. Springer-Verlag, New York, p. 471.

Wilson, T.H., Smith, V., Brown, A.L., 2013. Characterization of Tensleep reservoir fracture systems using outcrop analog, fracture image logs and 3D seismic. In: AAPG Rocky Mountain Section Meeting, Search and Discovery Article.